IEEE Photonics Journal
An IEEE Photonics Society Publication

Birefringence-Induced Trains of High-Rate Pulses in a Mode-Locked Fiber Laser

Volume 1, Number 2, August 2009

Avi Zadok
Jacob Sendowski
Amnon Yariv, Life Fellow, IEEE

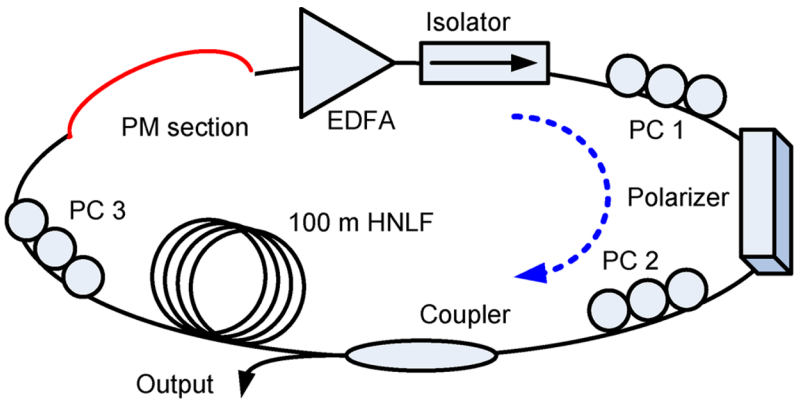

DOI: 10.1109/JPHOT.2009.2027441
1943-0655/$26.00 ©2009 IEEE

Birefringence-Induced Trains of High-Rate Pulses in a Mode-Locked Fiber Laser

Avi Zadok, Jacob Sendowski, and Amnon Yariv, *Life Fellow, IEEE*

Department of Applied Physics, California Institute of Technology, Pasadena, CA 91125 USA

DOI: 10.1109/JPHOT.2009.2027441
1943-0655/$26.00 ©2009 IEEE

Manuscript received June 8, 2009; revised July 1, 2009. First published Online July 7, 2009. Current version published July 24, 2009. The work of A. Zadok is supported by a postdoctoral research fellowship from the Center for the Physics of Information at Caltech and by the Rothschild fellowship from Yad-Hanadiv Foundation, Jerusalem, Israel. Corresponding author: A. Zadok (e-mail: avizadok@caltech.edu).

Abstract: The output of a mode-locked erbium-doped ring fiber laser incorporating a section of a polarization-maintaining (PM) fiber is investigated in both numerical simulations and experiments. With proper inline polarization control, the laser can be set to emit a train of pulses, separated by the differential group delay of the PM section. Repetition rates as high as 500 GHz are experimentally observed. The results provide an added insight into the role of birefringence in mode-locked lasers based on nonlinear polarization rotation.

Index Terms: Fiber lasers, mode-locked lasers, picosecond phenomena.

1. Introduction

Optical pulsed sources, having repetition rates in excess of 100 GHz, are attractive for applications such as ultrafast optical communication and spectroscopy. Self-starting, passively mode-locked fiber lasers have been favorable candidates for the realization of such sources, due to their simplicity, robustness and broad gain bandwidth, and the availability of high-power pump laser diodes [1]–[5]. One common underlying mode-locking technique used in these fiber lasers is based on intensity-dependent changes to the state of polarization (SOP) of a propagating waveform, referred to as nonlinear polarization rotation (NLPR) [6]–[8]. In conjunction with a properly aligned polarizer, NLPR represents an effective instantaneous saturable absorber, favoring the transmission of short, high-peak-power pulses [1], [9], [10].

A mode-locked laser can be configured to emit envelopes (trains) of high-repetition-rate pulses, by introducing a spectrally periodic inline filter. The filter selects a few frequency bands, spaced by its free spectral range $\Delta\nu$, that experience the least propagation loss [5]. These filtered spectral components may give rise to additional frequency bands, phase locked to the primary ones through a four-wave-mixing (FWM) process [1], [5], [11]. The resulting time-domain waveform is that of periodic pulses, separated by $1/\Delta\nu$. Using this technique, passively generated trains of high-rate pulses have been demonstrated in both anomalous and normal dispersion regimes [4]. In previous works, filtering elements included Fabry–Perot etalons [4], [12], [13], superimposed fiber Bragg gratings [5], [14], [15], and a Michelson interferometer [16].

A birefringent medium, such as a section of a polarization-maintaining (PM) fiber, in combination with a polarizer already included in the NLPR architecture, can also provide periodic spectral filtering. However, to the best of our knowledge, the generation of trains of high-repetition-rate pulses based on birefringence has not yet been attempted. Periodic features observed in the output power autocorrelation traces of NLPR mode-locked lasers have been previously attributed to

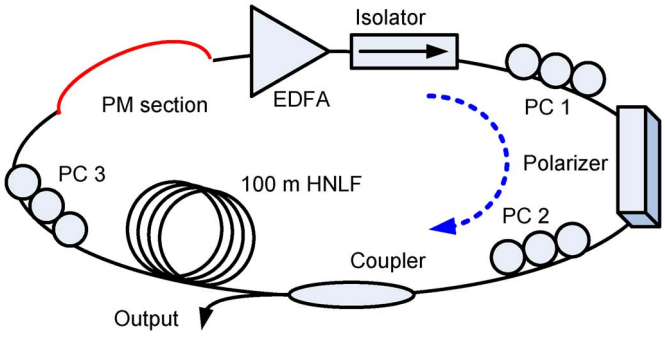

Fig. 1. A schematic drawing of the fiber laser system. The EDFA contains a pump laser diode, a pump beam combiner, and a section of erbium-doped fiber.

residual birefringence in erbium-doped fibers [17], [18]. However, the differential group delay (DGD) associated with the residual birefringence not being known, a quantitative account of the observed periodicity could not be provided.

In this paper, we revisit the role of birefringence in NLPR mode-locked fiber lasers, in order to quantitatively relate the observed pulse periodicity to the DGD. To this end, we study the operation of a fiber laser, with an inline PM section whose DGD is known and longer than that associated with the residual birefringence of all other components. We observe several regimes of mode-locked operation, such as single pulse operation or bursts of noise-like pulses [17], in both numerical simulations and experiments. Transition between different regimes is achieved through polarization control inside the fiber loop. This work focuses on a particular regime of operation, in which the laser is set to emit bursts of quasi-periodic pulses, separated by the DGD of the PM section. Our analysis provides approximate predictions for the polarization controller (PC) settings required for generating trains of high-repetition-rate pulses, which are supported by numerical simulations. The experimentally observed repetition rates are as high as 500 GHz. The results provide an added insight into the role of birefringence in NLPR mode locking and substantiate the previous suggestions of a birefringence-induced periodic output.

The remainder of this paper is organized as follows: Section 2 describes the principle of operation and simulations of the fiber laser, Section 3 provides experimental results, concluding remarks being given in Section 4.

2. Analysis and Simulations

A schematic drawing of the fiber laser system under study is shown in Fig. 1. The ring cavity includes an erbium-doped fiber amplifier (EDFA), characterized by its small signal power gain G_0, saturation power P_{sat}, optical frequency of maximal gain ω_0, spectral full width at half maximum BW and noise figure NF. The EDFA consists of a pump laser diode, a pump combiner and a section of erbium-doped fiber. An optical isolator at the EDFA output guarantees the unidirectional operation of the fiber laser. NLPR is realized via a polarizer, placed in between two PCs. Most of the cavity length is taken by a highly nonlinear fiber (HNLF), whereas the PCs and connecting patch cords are of standard single-mode fiber (SMF). A 10% tapping coupler is placed prior to the HNLF, providing the laser output. Spectral filtering is introduced by a PM section of DGD τ, preceded by yet another PC. Both the HNLF and the SMF sections display a residual birefringence. While much weaker than that of the PM section, this residual birefringence is significant in nonlinear pulse propagation. Nonlinear propagation effects and dispersion within the relatively short erbium-doped and PM fiber sections are neglected.

Even though the laser output must be solved for numerically, an insight into the filtering effect of the PM section, and approximate alignments of the PCs which lead to different regimes of operation, can be obtained from simplistic, illustrative considerations. In the following qualitative argument, we temporarily ignore the SMF section and the dispersion in the HNLF section, which is

nearly zero. We follow the propagation of the lasing waveform at the steady state for a complete loop cycle along the fiber ring cavity, starting at the HNLF input (see Fig. 1). Let us denote the two axes of the residual birefringence in the HNLF as $\hat{e}_1^{HNLF}$ and $\hat{e}_2^{HNLF}$, and suppose that the optical field at the HNLF input is linearly polarized at an angle θ_1 with respect to $\hat{e}_1^{HNLF}$. The field at the HNLF output becomes elliptically polarized, with a nonlinear-propagation-induced differential phase between the field components aligned with $\hat{e}_1^{HNLF}$ and $\hat{e}_2^{HNLF}$. Subject to the above simplifying assumptions, that differential phase at the peak of the propagating waveform is given by [19]

$$\Delta\varphi_{NL} = \frac{1}{3} P \gamma_{HNLF} L_{HNLF} \cos(2\theta_1). \tag{1}$$

In Eq. (1), P denotes the peak power, γ_{HNLF} is the nonlinear coefficient of the HNLF in units of $[\mathrm{W}\cdot\mathrm{km}]^{-1}$, and L_{HNLF} is the HNLF length. We may adjust PC3 so that $\hat{e}_1^{HNLF}$ and $\hat{e}_2^{HNLF}$ are mapped to the principal axes $\hat{e}_1^{PM}$ and $\hat{e}_2^{PM}$ of the PM section, respectively. Propagation through the PM section introduces a frequency-dependent, additive differential phase between the two field components: $\Delta\varphi_{PM} = \Delta\omega \cdot \tau$, with $\Delta\omega$ the detuning from ω_0. The optical power of both field components is amplified by the net steady state EDFA gain $G(\Delta\omega)$, which is assumed to be polarization independent. At the polarizer input, $\hat{e}_1^{PM}$ is mapped to a different SOP, aligned at some angle θ_2 with respect to the transmission axis of the polarizer. We may configure PC1 to obtain $\theta_2 = \pi/2 - \theta_1$, and PC2 to recover the original, linear SOP at the HNLF input. A propagation cycle along the fiber ring is thus completed. With the above alignments, the optical power transfer function of the full propagation cycle can be roughly approximated by

$$T_{App}(\Delta\omega) \approx \frac{1}{2} G(\Delta\omega) \sin^2(2\theta_1)[1 - \cos(\Delta\omega \cdot \tau + \Delta\varphi_{NL} + \Delta\varphi_{Lin})]. \tag{2}$$

Here, $\Delta\varphi_{Lin}$ is a linear-propagation-induced differential phase, which is affected, among other factors, by the states of the PCs.

The above expression provides only a limited approximation, since $\Delta\varphi_{NL}$ is not constant throughout the waveform and dispersion effects have been neglected. Nonetheless, it could be useful for identifying certain properties of the system. The combination of the PM section DGD and the polarizer represents an effective optical filter, whose transfer characteristics depend on both the settings of PCs, (through $\Delta\varphi_{Lin}$), and on the power of the propagating waveform, (through $\Delta\varphi_{NL}$). At steady state lasing operation, we expect the maximum value of the approximate loop transfer function to be near unity: $\max[T_{App}(\Delta\omega)] \approx 1$. An alignment of the PCs leading to $\Delta\varphi_{Lin} = -\Delta\varphi_{NL}$ would favor two transmission peaks at $\Delta\omega = \pm\pi/\tau$, which in turn could give rise to trains of pulses separated by τ through NLPR mode locking. We therefore expect that a more complete, numeric solution for the laser would include a regime of output bursts consisting of equally spaced pulses.

In place of Eq. (1), the propagation through both the HNLF and SMF sections was modeled by numerically solving a set of two coupled equations, incorporating second-order linear dispersion, self-phase-modulation, and polarization cross phase modulation [6]–[8]

$$\begin{aligned} \partial A_{1,F}/\partial z + \frac{j}{2}\beta''_F \partial^2 A_{1,F}/\partial t^2 &= j\gamma_F \left(|A_{1,F}|^2 + \frac{2}{3}|A_{2,F}|^2 \right) A_{1,F} \\ \partial A_{2,F}/\partial z + \frac{j}{2}\beta''_F \partial^2 A_{2,F}/\partial t^2 &= j\gamma_F \left(|A_{2,F}|^2 + \frac{2}{3}|A_{1,F}|^2 \right) A_{2,F} \end{aligned} \tag{3}$$

where $A_{1,F}$ and $A_{2,F}$ denote the complex envelopes of the electrical field components along the principal axes of residual birefringence 1 and 2 of a fiber section, and the subscript F denotes either *HNLF* or *SMF*, for the HNLF or SMF sections, respectively. The fields depend on both time t and longitudinal position z. The length, second-order dispersion coefficient and nonlinear coefficient of

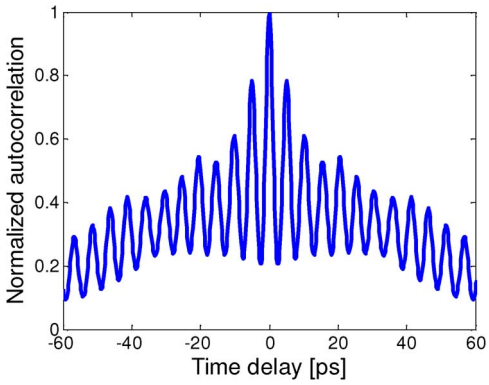

Fig. 2. Example of the simulated, normalized autocorrelation of the laser output power. The simulation parameters are $L_{HNLF} = 100$ m, $\beta''_{HNLF} = -1.5$ ps^2/km, $\gamma_{HNLF} = 11.3$ (W · km)$^{-1}$ $L_{SMF} = 50$ m, $\beta''_{SMF} = -21$ ps^2/km, $\gamma_{SMF} = 1.3$ (W · km)$^{-1}$, $P_{sat} = 20$ mW, $G_0 = 20$ dB, $NF = 6$ dB, $BW = 4.5$ nm, and $\tau = 5$ ps. Linear and coupling losses in the cavity for one cycle were 4 dB.

the HNLF (SMF) are denoted by $L_{HNLF}(L_{SMF})$, $\beta''_{HNLF}(\beta''_{SMF})$ and $\gamma_{HNLF}(\gamma_{SMF})$, respectively. We consider L_{HNLF} and L_{SMF} that are longer than the beat lengths L_B of the residual birefringence in the respective sections (typically $L_B \sim 20$ m). In this limit, terms of the form $j/3\gamma A_1^* A_2^2 \exp(-4\pi j z/L_B)$, which would appear in equation (3) in the most general case, can be neglected [7]. The PM fiber section was once again modeled by the differential phase $\Delta\varphi_{PM} = \Delta\omega \cdot \tau$, as discussed above. The initial condition for the laser output calculation was the spontaneous emission field of the EDFA.

Fig. 2 shows an example of the calculated autocorrelation of the laser output power. The simulations parameters were $L_{HNLF} = 100$ m, $\beta''_{HNLF} = -1.5$ ps^2/km, $\gamma_{HNLF} = 11.3$(W·km)$^{-1}$ $L_{SMF} = 50$ m, $\beta''_{SMF} = -21$ ps^2/km, $\gamma_{SMF} = 1.3$(W · km)$^{-1}$, $P_{sat} = 20$ mW, $G_0 = 20$ dB, $NF = 6$ dB, $BW = 4.5$ nm, and $\tau = 5$ ps. Fiber lengths on the same scale were used in previous works [17], [18]. The overall linear propagation and coupling losses in the ring were 4 dB per cycle. With proper alignment of the PCs, the steady state laser output is a burst of periodic pulses, separated by τ, as anticipated. The duration of each burst is on the order of 100 ps, with peak power levels of several W. PC alignments which provide steady state output bursts with substantial output periodicity are typically characterized by $\max[T_{App}(\Delta\omega)]$ between 1.3 and 1.6, and $|\Delta\varphi_{Lin} + \Delta\varphi_{NL}| \leq 0.3$ rad. The simplistic propagation analysis, therefore, provides useful initial PC settings for investigating the system characteristics.

3. Experiment

An NLPR mode-locked fiber laser with an intracavity PM section was investigated in a proof-of-principle experiment. The laser ring structure was the same as that of Fig. 1, and the parameters of the EDFA and the various fiber sections in the experiment were the same as those of the simulations above, except for interchangeable PM fiber sections of varying DGD values. The PM fiber used had a beat length of 4 mm, which corresponds to a DGD of 1.3 ps per 1 m of fiber at a wavelength of 1550 nm. The DGD associated with the birefringence of the HNLF and SMF sections is estimated as lower than 0.2 ps/km$^{0.5}$. The mean output-coupled power of the laser was of the order of 0.5–1 mW. Fig. 3(a) shows an oscilloscope trace of the detected output power. Output bursts are observed, separated by the cavity propagation delay of 840 ns.

Fig. 3(b) shows an example of the normalized, measured autocorrelation trace of the laser output power, obtained with a DGD of $\tau = 5.5$ ps. Periodic peaks separated by τ are clearly observed. The periodic modulation in the autocorrelation trace appears shallow, due to the long averaging time of the available autocorrelator in a relatively long, fast sweep of the relative delay. The inset of the figure shows a slower, short-range autocorrelation scan of the output power, taken at the same PCs settings, showing the modulation to be in fact much more pronounced. The asymmetry of the traces

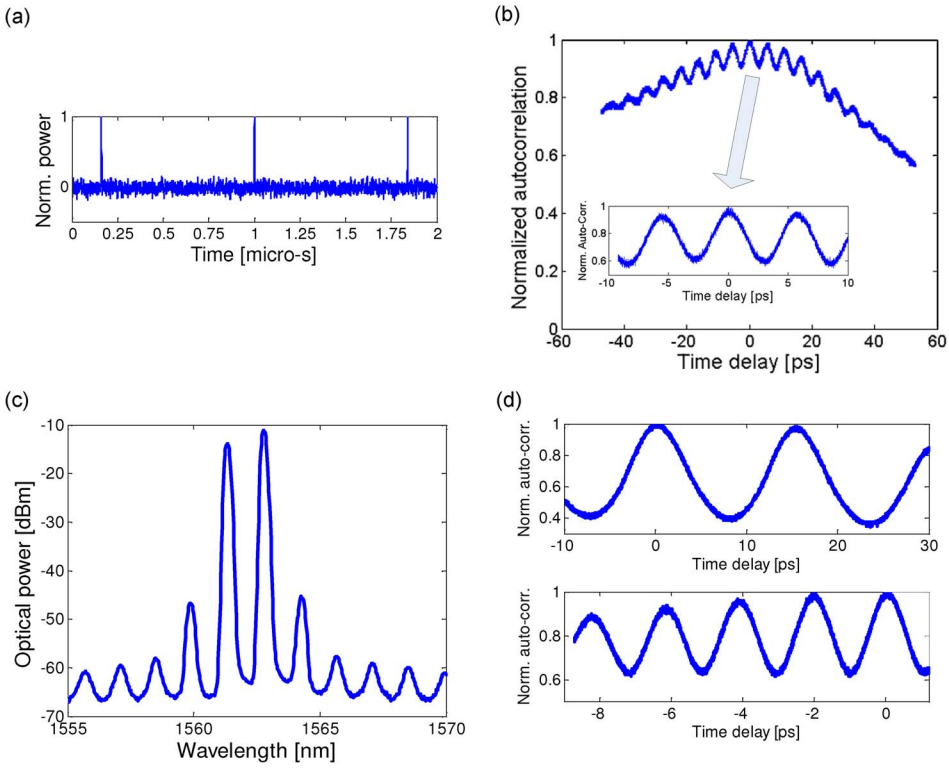

Fig. 3. Experimental results. The EDFA and fiber sections parameters are the same as those of Fig. 2, except for a varying τ. (a) Measured normalized output power as a function of time, indicating mode-locked output bursts. (b) Example of measured, normalized autocorrelation of the output power, taken with $\tau = 5.5$ ps. The inset shows a high-resolution, short-range autocorrelation scan. (c) Measured optical power spectrum, corresponding to the autocorrelation trace of panel (b). (d) Examples of measured, normalized autocorrelation of the output power for (top) $\tau = 16$ ps and (bottom) $\tau = 2$ ps.

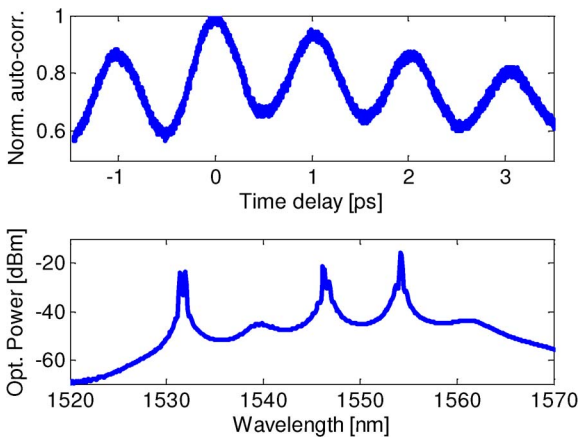

Fig. 4. Example of (top) measured, normalized autocorrelation of the output power and (bottom) optical power spectrum for a fiber laser with no PM section. The EDFA and other fiber sections parameters are the same as those of Figs. 2 and 3.

can suggest an asymmetry in the burst shape, but may also be due to alignment difficulties inside the autocorrelator. Fig. 3(c) shows the optical power spectrum corresponding to Fig. 3(b). As expected, the periodic autocorrelation is associated with two spectral peaks of nearly equal power, separated by $1/\tau$. Similar results were obtained for two other DGD values: $\tau = 2$, 16 ps, with examples of periodic output power autocorrelation given in Fig. 3(d). Finally, the output of the laser with no

PM section was examined as well. Even without an intentionally introduced DGD, periodic output features could be obtained through careful adjustments of the PCs, as previously reported [17], [18] (see Fig. 4). The period of 1 ps could represent the residual birefringence of the EDFA in the loop.

4. Summary

A mode-locked fiber ring laser with an inline PM section was investigated. Mode locking was obtained based on NLPR and an inline polarizer. In conjunction with the DGD of the PM section, the polarizer takes up the added functionality of a periodic spectral filter. The interplay of mode locking and filtering was studied in both numerical simulations and experiments. It was shown that the laser can be set to emit bursts of periodic pulses, separated by the PM section DGD. This regime of operation is associated with two dominant spectral peaks of comparable magnitudes. Repetition rates as high as 500 GHz were obtained. To the best of our knowledge, the passive generation of high-repetition-rate pulses based on birefringence has not been directly demonstrated to date.

Compared with other inline filtering mechanisms [4], [5], [12]–[16], the spectral selectivity provided by a single PM section is relatively weak. Each of the spectral bands, therefore, has a relatively broad envelope, consisting of a large number of individual, longitudinal modes that are locked together. The duration of the corresponding temporal envelope is inversely proportional to the width of each spectral band, and is thus relatively short. Higher order filtering can be achieved via concatenating several PM sections [20]. The low saturation power of the available EDFA may also restrict the number of pulses supported by the laser. In addition, the long-term stability of states of polarization along a fiber loop, not investigated in this work, may become a concern. The principle described in this work could be carried into waveguide-based implementation of race-track configuration lasers containing birefringence, which are better suited for polarization stability. In addition, the results provide strong quantitative support to the previously suggested role of residual birefringence in passive, high-repetition-rate pulse generation [17], [18].

Acknowledgment

The authors wish to thank Prof. B. Crosignani of the California Institute of Technology (Caltech) and Universita' dell'Aquila, Italy, for useful discussions and for reading the manuscript.

References

[1] G. P. Agrawal, *Applications of Nonlinear Fiber Optics,* 2nd ed., New York: Academic, 2008.
[2] P. Franco, F. Fontana, I. Cristiani, M. Midrio, and M. Romagnoli, "Self-induced modulation-instability laser," *Opt. Lett.*, vol. 20, no. 19, pp. 2009–2011, Oct. 1995.
[3] C. J. S. de Matos, D. A. Chestnut, and J. R. Taylor, "Low-threshold self-induced modulation instability ring laser in highly nonlinear fiber yielding a continuous wave 262-GHz soliton train," *Opt. Lett.*, vol. 27, no. 11, pp. 915–917, Jun. 2002.
[4] T. Sylvestre, S. Coen, P. Emplit, and M. Haelterman, "Self-induced modulation instability laser revisited: Normal dispersion and dark-pulse train generation," *Opt. Lett.*, vol. 27, no. 7, pp. 482–484, Apr. 2002.
[5] J. Schroder, S. Coen, F. Vanholsbeeck, and T. Sylvestre, "Passively mode-locked Raman fiber laser with 100 GHz repetition rate," *Opt. Lett.*, vol. 31, no. 23, pp. 3489–3491, Dec. 2006.
[6] B. Crosignani and P. Di Porto, "Intensity induced rotation of the polarization ellipse in low-birefringence single-mode optical fibers," *J. Mod. Opt. (Optica Acta)*, vol. 32, no. 9/10, pp. 1251–1258, Sep. 1985.
[7] G. P. Agrawal, *Nonlinear Fiber Optics,* 4th ed. New York: Academic, 2007, p. 180.
[8] A. Yariv and P. Yeh, *Photonics,* 6th ed. London, U.K.: Oxford Univ. Press, 2007, p. 640.
[9] K. Tamura, H. A. Haus, and E. Ippen, "Self-starting additive pulse mode-locked erbium fibre ring laser," *Electron. Lett.*, vol. 28, no. 24, pp. 2226–2228, Nov. 1992.
[10] K. Tamura, E. P. Ippen, H. A. Haus, and L. E. Nelson, "77-fs pulse generation from a stretched-pulse mode-locked all-fiber ring laser," *Opt. Lett.*, vol. 18, no. 13, pp. 1080–1082, Jul. 1993.
[11] M. Quiroga-Teixeiro, C. Balslev Clausen, M. P. Sorensen, P. L. Christiansen, and P. A. Andrekson, "Passive mode locking by dissipative four-wave mixing," *J. Opt. Soc. Amer. B, Opt. Phys.*, vol. 15, no. 4, pp. 1315–1321, Apr. 1998.
[12] E. Yoshida and M. Nakazawa, "Low-threshold 115-GHz continuous-wave modulational-instability erbium-doped fiber laser," *Opt. Lett.*, vol. 22, no. 18, pp. 1409–1411, Sep. 1997.
[13] P. Honzatko, P. Peterka, and J. Kanka, "Modulational-instability σ-resonator fiber laser," *Opt. Lett.*, vol. 26, no. 11, pp. 810–812, Jun. 2001.

[14] S. Zhang, F. Lu, X. Dong, P. Shum, X. Yang, X. Zhou, Y. Gong, and C. Lu, "Passive mode locking at harmonics of the free spectral range of the intracavity filter in a fiber ring laser," *Opt. Lett.*, vol. 30, no. 21, pp. 2852–2854, Nov. 2005.
[15] J. Schroder, D. Alasia, T. Sylvestre, and S. Coen, "Dynamics of an ultrahigh-repetition-rate passive mode-locked Raman fiber laser," *J. Opt. Soc. Amer. B, Opt. Phys.*, vol. 25, no. 7, pp. 1178–1186, Jul. 2008.
[16] J. M. Sousa and O. G. Okhotnikov, "Short pulse generation and control in Er-doped frequency-shifted-feedback fibre lasers," *Opt. Commun.*, vol. 183, no. 1–4, pp. 227–241, Sep. 2000.
[17] M. Horowitz and Y. Silberberg, "Control of noiselike pulse generation in erbium-doped fiber lasers," *IEEE Photon. Technol. Lett.*, vol. 10, no. 10, pp. 1389–1391, Oct. 1998.
[18] M. J. Guy, D. U. Noske, and J. R. Taylor, "Generation of femtosecond soliton pulses by passive mode locking of an ytterbium-erbium figure-of-eight fiber laser," *Opt. Lett.*, vol. 18, no. 17, pp. 1447–1449, Sep. 1993.
[19] Z. Chen, H. Sun, S. Ma, and N. K. Dutta, "Dual-wavelength mode-locked erbium-doped fiber ring laser using highly nonlinear fiber," *IEEE Photon. Technol. Lett.*, vol. 20, no. 24, pp. 2066–2068, Nov./Dec. 2008.
[20] A. Eyal, "Synthesis and characterization of broad-band polarization-mode dispersion equalizers," *J. Lightw. Technol.*, vol. 22, no. 4, pp. 1147–1154, Apr. 2004.